Scripta Materialia 144 (2018) 1–4

Contents lists available at ScienceDirect

Scripta Materialia

journal homepage: www.elsevier.com/locate/scriptamat

Regular article

Evidence of 3D strain gradients associated with tin whisker growth

Johan Hektor[a,*], Jean-Baptiste Marijon[b], Matti Ristinmaa[a], Stephen A. Hall[a], Håkan Hallberg[a], Srinivasan Iyengar[c], Jean-Sébastien Micha[d,e], Odile Robach[d,f], Fanny Grennerat[g], Olivier Castelnau[b]

[a] Division of Solid Mechanics, Lund University, Box 118, Lund 221 00, Sweden
[b] Laboratory PiMM, UMR CNRS 8006, Arts & Métiers ParisTech – CNAM, Paris, France
[c] Division of Materials Engineering, Lund University, Box 118, Lund 221 00, Sweden
[d] CEA-CNRS CRG-IF BM32 Beamline at ESRF, Grenoble, France
[e] Université Grenoble Alpes, INAC-SPrAM and CNRS, SPrAM and CEA, INAC-SPrAM, PCI, Grenoble, France
[f] Université Grenoble Alpes, INAC-SP2M and CEA, INAC-SP2M, NRS, Grenoble, France
[g] LGT Argouges, Éducation Nationale, Grenoble, France

ARTICLE INFO

Article history:
Received 18 August 2017
Received in revised form 18 September 2017
Accepted 18 September 2017
Available online xxxx

Keywords:
Whiskers
Intermetallic compounds
Lead-free solder
X-ray diffraction

ABSTRACT

We have used Differential Aperture X-ray Microscopy (DAXM) to measure grain orientations and deviatoric elastic strains in 3D around a tin whisker. The results show strain gradients through the depth of the tin coating, revealing a higher strain deeper in the Sn layer. These higher strains are explained by the volume change occurring during growth of the intermetallic phase Cu_6Sn_5 at the interface between the Cu substrate and the Sn coating and at grain boundaries between Sn grains.

Tin whiskers are filamentary tin grains, only a few micrometers wide, but capable of growing to several millimeters in length. Whiskers grow spontaneously from tin coated surfaces and are electrically conducting. This may cause issues due to short-circuiting between components of electronic devices. A number of failures of electronic products due to short circuiting caused by whisker growth have been reported [1]. Until recently, the problem of whisker growth was effectively solved by using Pb–Sn alloys rather than pure Sn. However, due to environmental concerns this solution is no longer available. The ban on the use of lead in electronic devices and components, combined with the current trend of miniaturization, can be envisaged to increase the problems caused by whisker growth in the near future.

Tin whiskers have been an active area of research for over 60 years [2]. Despite this, several questions remain to be resolved regarding the mechanisms causing the whiskers to form and grow. The main hypothesis is that whiskers grow to relax stresses in the tin layer [2–5]. In the case of tin coatings on copper substrates, which is the system studied in this work, the stress is often associated with the volume change caused by the formation and growth of the intermetallic phase Cu_6Sn_5. It has been shown both experimentally [6–9] and by numerical simulations [10,11] that the growth of Cu_6Sn_5 at the interface between the Sn layer and the Cu substrate and at grain boundaries between Sn grains generates compressive stress in the tin layer. However, formation of intermetallic phases is not a necessary condition for whisker growth. Williams et al. [12] report whisker growth on Sn–W samples not forming intermetallic phases. Sobiech et al. [13,14] and Sun et al. [15] claim that the state of stress (tensile or compressive) is unimportant for whisker growth. Instead, they argue that whisker growth is driven by negative strain gradients in the tin layer, i.e. that the strain at the root of the whisker should be more tensile/less compressive than in the surrounding microstructure.

Previous X-ray diffraction studies of tin whiskers have used techniques that only provide spatial resolution in the two dimensions parallel to the Sn coating [4,14,16-18]. This means that the results are averaged over the penetration depth of the X-rays, which is typically on the order of 10 µm. By using Differential Aperture X-ray Microscopy (DAXM) [19–21] diffraction patterns from different depths in a sample can be reconstructed, thus obtaining spatial resolution in three dimensions. This makes it possible to study the grain structure and the strain field around whiskers in greater detail.

* Corresponding author.
E-mail address: johan.hektor@solid.lth.se (J. Hektor).

https://doi.org/10.1016/j.scriptamat.2017.09.030

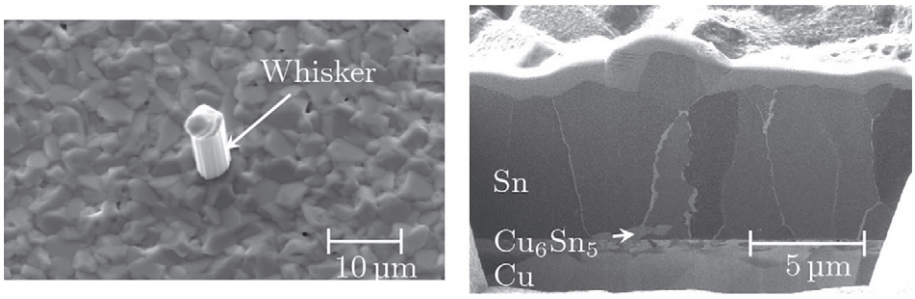

Fig. 1. Left: SEM image of the tin whisker selected for the microdiffraction measurements. Right: FIB cross section showing the columnar grain structure of the Sn layer and the formation of Cu_6Sn_5 at the Cu–Sn interface and at grain boundaries between Sn grains.

In the present work, tin coatings with a thickness of approximately 6.5 μm were deposited on polished 1 mm thick Cu sheets by means of electron beam evaporation. The microstructure of the Sn layer consists of columnar grains, typical for Sn coatings [7,22,23], see Fig. 1. After deposition, the samples were left to age for four months under ambient conditions during which whisker formation took place. Prior to the X-ray experiment, a suitable whisker was located using a scanning electron microscope, see Fig. 1.

The X-ray measurements were performed using the Laue microdiffraction setup on the CRG-IF BM32 beamline at the European Synchrotron Radiation Facility (ESRF) [24]. A polychromatic X-ray beam of 5–23 keV was focused to a spot of 0.7 μm size on the sample using a pair of Kirkpatrick-Baez (KB) mirrors. The sample was mounted at an angle of 40° with respect to the incoming beam and the diffracted X-rays were measured by a Mar CCD 2D detector comprising 2048 × 2048 pixels with a pixel size of about 80 μm, placed at an angle of 90° with respect to the incident beam. This geometry allowed for measurements of reflections in the range $41^\circ \leq 2\theta \leq 139^\circ$.

Conventional Laue microdiffraction can provide information about the crystal structure, orientation, and deviatoric elastic strains of a sample. Due to the penetration depth of the X-rays, the measurements are averaged over the volume probed by the beam [18]. Furthermore, strain determination is less accurate for grains below the surface of the sample. To remedy these limitations, a wire acting as a 'differential-aperture' can be placed between the sample and the detector [19], the experimental setup for DAXM measurements is illustrated in Fig. 2. During the measurement the wire is moved in 1 μm steps parallel to the sample surface and a diffraction pattern is measured for each wire position. By comparing the differential intensity of given detector pixels between two successive wire positions, it is possible to determine the scattering contribution as a function of depth along the beam [20]. The resolution in depth is essentially governed by the distances between the wire, the incident beam and the detector, by the number of steps scanned with the wire, the scanning direction, and (an effect neglected here) by the non-zero transmission of the wire edges [21].

The measured diffraction patterns were analyzed using the LaueTools software [25], being developed at the BM32 synchrotron beamline. The depth-resolved diffraction patterns can be indexed to obtain the crystallographic orientation of each of the grains illuminated by the X-rays. For each reciprocal unit cell an orientation matrix describing the orientation of the unit cell is obtained. From the orientation matrix the direct, $(a, b, c, \alpha, \beta, \gamma)$, and reciprocal, $(a^*, b^*, c^*, \alpha^*, \beta^*, \gamma^*)$, lattice parameters of the deformed crystal can be extracted. Following Ice and Pang [26], the elastic strains, in a frame attached to the crystal lattice and assuming small deformations, can be calculated as

$$\boldsymbol{\varepsilon} = \frac{1}{2}\left(\boldsymbol{A}\boldsymbol{A}_0^{-1} + \left(\boldsymbol{A}\boldsymbol{A}_0^{-1}\right)^T\right) - \boldsymbol{I}, \tag{1}$$

with $\boldsymbol{I}$ being the identity matrix and

$$\boldsymbol{A} = \begin{bmatrix} a & b\cos\gamma & c\cos\beta \\ 0 & b\sin\gamma & -c\sin\beta\cos\alpha^* \\ 0 & 0 & c\sin\beta\sin\alpha^* \end{bmatrix}. \tag{2}$$

the matrix $\boldsymbol{A}_0$ in Eq. (1) is constructed as in Eq. (2) but using the lattice parameters of an unstrained crystal. Unstrained Sn has a body-centered tetragonal structure with lattice parameters $a = b = 5.83$ Å, $c = 3.18$ Å and $\alpha = \beta = \gamma = 90^\circ$ [4]. Since each Laue spot is related to a unique family of lattice planes, variation of the angles between Laue spots directly corresponds to the strain of the unit cell. However, due to the polychromatic beam used in the experiment, it is not possible to determine the volume of the unit cell. For this reason only the deviatoric part of the elastic strain tensor can be determined,

$$\boldsymbol{\varepsilon}^{dev} = \boldsymbol{\varepsilon} - \frac{1}{3}\mathrm{tr}(\boldsymbol{\varepsilon})\boldsymbol{I}, \tag{3}$$

where $\mathrm{tr}(\boldsymbol{\varepsilon})$ denotes the trace of the strain tensor. The effective strain, which is an invariant of the strain tensor, is defined by

$$\varepsilon_{eff} = \sqrt{\frac{2}{3}\boldsymbol{\varepsilon}^{dev} : \boldsymbol{\varepsilon}^{dev}}, \tag{4}$$

with : denoting the double contraction operator.

Two orthogonal lines, 8 μm and 16 μm long, intersecting at the whisker root, were scanned at steps of 0.8 μm using DAXM. In Fig. 3, the reconstruction in depth of four diffraction peaks belonging to two different Sn grains is shown. The diffraction patterns were reconstructed with 1 μm resolution in depth. The first two rows of the figure show Laue spots coming from a grain at the surface of the sample, while the lower two rows show spots from a grain beneath the

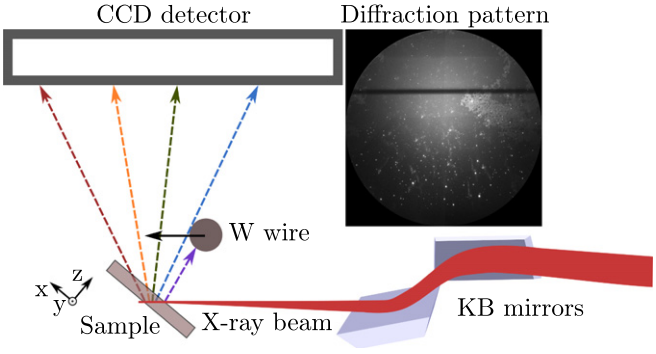

Fig. 2. Schematic view of the experimental setup for Laue microdiffraction. The W wire is only used during the 3D measurements. The wire is seen as a horizontal shadow on the diffraction pattern.